

SCIENTIFIC REPORTS



OPEN

Genomic Identification and Comparative Expansion Analysis of the *Non-Specific Lipid Transfer Protein* Gene Family in *Gossypium*

Feng Li^{1,*}, Kai Fan^{1,2,*}, Fanglu Ma¹, Erku Yue¹, Noreen Bibi^{1,3}, Ming Wang¹, Hao Shen¹, Md Mosfeq-Ul Hasan¹ & Xuede Wang¹

Received: 02 June 2016
Accepted: 16 November 2016
Published: 15 December 2016

Plant non-specific lipid transfer proteins (nsLTPs) are involved in many biological processes. In this study, 51, 47 and 91 nsLTPs were identified in *Gossypium arboreum*, *G. raimondii* and their descendant allotetraploid *G. hirsutum*, respectively. All the nsLTPs were phylogenetically divided into 8 distinct subfamilies. Besides, the recent duplication, which is considered cotton-specific whole genome duplication, may have led to nsLTP expansion in *Gossypium*. Both tandem and segmental duplication contributed to nsLTP expansion in *G. arboreum* and *G. hirsutum*, while tandem duplication was the dominant pattern in *G. raimondii*. Additionally, the interspecific orthologous gene pairs in *Gossypium* were identified. Some GaLTPs and GrLTPs lost their orthologs in the A_t and D_t subgenomes, respectively, of *G. hirsutum*. The distribution of these GrLTPs and GaLTPs within each subfamily was complementary, suggesting that the loss and retention of nsLTPs in *G. hirsutum* might not be random. Moreover, the nsLTPs in the A_t and D_t subgenomes might have evolved symmetrically. Furthermore, both intraspecific and interspecific orthologous genes showed considerable expression variation, suggesting that their functions were strongly differentiated. Our results lay an important foundation for expansion and evolutionary analysis of the nsLTP family in *Gossypium*, and advance nsLTP studies in other plants, especially polyploid plants.

Lipids play a vital role in plant growth and development. They can maintain cell function and mediate cell signaling associated with stress responses. Plant non-specific lipid transfer proteins (nsLTPs) (6.5–10.5 kDa in size) are able to transfer phospholipids and fatty acids between membranes *in vitro*^{1,2}. They are abundantly present in various plants, representing up to 4% of the total soluble protein². These peptides are structurally characterized by an eight cysteine motif (8 CM) backbone with the general form C-Xn-C-Xn-CC-CXC-Xn-C-Xn-C, and the cysteine residues are linked by four disulfide bonds to stabilize a tertiary structure of a hydrophobic cavity^{2,3}. Moreover, almost all nsLTPs carry an N-terminal secretory signal peptide (21–27 amino acids in length) in their nascent polypeptides, indicating that they are secreted proteins^{2,4}. In previous studies, plant nsLTPs have been identified to participate in a range of biological processes, including cuticular wax and cutin synthesis, biotic and abiotic stress resistance, plant signaling, seed maturation and sexual reproduction^{2,4}. In some cases, nsLTPs are considered pathogenesis-related (PR) proteins and constitute the PR-14 family⁵. The defensive role of plant nsLTPs against fungal, bacterial and viral pathogens has been well verified by ample evidence^{2,6–8}.

Plant nsLTPs have been well studied and identified in many plant species including both flowering and non-flowering plants². They were initially classified into two types according to molecular mass: nsLTP1 (9 kDa) and nsLTP2 (7 kDa)¹. The disulfide bond linkages of nsLTP1 at Cys₁-Cys₆ and Cys₅-Cys₈ differ from those of nsLTP2 at Cys₁-Cys₅ and Cys₆-Cys₈. Recently, a new classification according to sequence similarity and intervals of 8 CM was proposed by Boutrot *et al.*³. The system categorized 267 nsLTPs into nine types (Type I-IX) based on a genome-wide analysis of rice (*Oryza sativa*), wheat (*Triticum aestivum*) and *Arabidopsis thaliana*. Then, nsLTPs

¹Institute of Crop Science, College of Agriculture and Biotechnology, Zhejiang University, Hangzhou 310058, People's Republic of China. ²College of Crop Science, Fujian Agriculture and Forestry University, Fuzhou, 350002, Fujian, China. ³Nuclear Institute for Agriculture and Biology, Faisalabad, Pakistan. *These authors contributed equally to this work. Correspondence and requests for materials should be addressed to X.W. (email: xdwang@zju.edu.cn)

in other plant species were also grouped according to Boutrot's method with slight modifications^{4,9–12}, and novel types such as Type X⁹ and Type XI⁴ were identified.

Cotton provides the world's most utilized natural fiber for the textile and garment industries. The genus *Gossypium* comprises approximately 45 diploid species and can be divided into eight monophyletic groups (each designated alphabetically as A through G, and K)^{13,14}. The A- and D- genome diploids diverged from the same eudicot progenitor approximately 5–10 million years ago (MYA). Then, ancient hybridization between A and D diploids occurred, resulting in the generation of a clade of five allotetraploid species approximately 1–2 MYA¹⁵. *Gossypium hirsutum* is one of the descendant allotetraploid species and may be derived from a spinnable fiber capable A genome species (*G. arboreum*) and a non-spinnable fiber capable D genome species (*G. raimondii*)^{15,16}. Cotton polyploidization has altered the function of the A and D ancestral diploid genomes and conferred emergent properties¹⁷. More than 90% of world cotton production is attributable to the cultivation of *G. hirsutum*¹⁵. However, a soil-borne vascular disease, *Verticillium* wilt, which is caused by *Verticillium dahliae*, is the most prevalent and lethal disease affecting cotton production. It is a critical plant quarantine disease and called the “cancer” of cotton crop¹⁸. Few *G. hirsutum* germplasms were found to be resistant to *V. dahliae*¹⁹. Comprehensive prevention and control measures are limited solely to improvements in genetic resistance^{19,20}.

In previous studies, only a small portion of nsLTPs from cotton have been characterized^{2,21,22}. With *G. raimondii*, *G. arboreum* and *G. hirsutum* genome sequencing completed^{14,15,23}, an excellent opportunity is coming to initiate whole-genome annotation and to perform comparative genomic study in *Gossypium*. Until now, a genome-wide overview of the nsLTP family in *Gossypium* has yet to be reported. Thus, a systematic molecular evolution and expansion analysis of the nsLTPs in *Gossypium* is urgently required. In this study, putative nsLTPs were identified in *G. raimondii*, *G. arboreum* and *G. hirsutum*. We conducted a comprehensive study on the phylogenetics, genomic structure, chromosomal localization and expansion history to evaluate the molecular evolution, expansion history and expression profiles of the nsLTP family in *Gossypium*.

Results

Genomic identification of putative nsLTPs in *G. raimondii*, *G. arboreum* and *G. hirsutum*. The availability of *G. raimondii*, *G. arboreum* and *G. hirsutum* genome sequences makes it possible to identify all the nsLTPs in the three *Gossypium* species. The BLASTP program was utilized to search for candidate nsLTPs in cotton with the query sequences from Arabidopsis. Initially, 104, 104 and 182 protein sequences were identified in *G. raimondii*, *G. arboreum* and *G. hirsutum*, respectively. After screening and selection as described in the materials and methods, a total of 189 nsLTPs were confirmed and described (Table S2). Among them, *G. raimondii* and *G. arboreum* contain a similar number of nsLTPs (47 and 51, respectively), despite the fact that *G. raimondii* has a much smaller genome size (885 Mb/1 C) than *G. arboreum* (1,746 Mb/1 C). In *G. hirsutum* (2,173 Mb), 91 nsLTPs were identified, representing almost a two-fold increase over the number of nsLTPs in its diploid progenitors. We designated the genes identified in *G. raimondii*, *G. arboreum* and *G. hirsutum* as GrLTPs, GaLTPs and GhLTPs, respectively.

Phylogenetic analysis of the nsLTP family. To determine the evolutionary relationships of nsLTPs, phylogenetic analysis of the identified nsLTPs in *Gossypium* and Arabidopsis was completed with the MrBayes and PHYMLIP tools (Fig. 1, Fig. S1). There were similar results with high support values from each method. According to Boutrot's classification system, the nsLTP family in *Gossypium* was divided into 8 subfamilies (Type I, II, III, IV, V, VI, VIII and IX), and no Type VII nsLTPs were identified in cotton (Fig. 1, Fig. S1, Table S2). The member proportion was different in each subfamily (Fig. S2a). The Type I subfamily (33.33%) contained the most members, followed by Type II (23.28%), Type V (16.93%) and Type IV (11.64%). The least represented subfamily was Type IX (1.59%). A similar member distribution in each subfamily was found in each *Gossypium* species (Fig. S2b). Besides, the proportion of nsLTPs in Type I was 35.29% and 38.30% in *G. arboreum* and *G. raimondii*, respectively, whereas it decreased to 29.67% in *G. hirsutum*. The proportion of members in both Type II and Type VIII in *G. hirsutum* (25.27% and 7.69%, respectively) was higher than that in *G. arboreum* (23.53% and 3.92%, respectively) and *G. raimondii* (19.15% and 4.26%, respectively). Moreover, not all the subgroups were present in each *Gossypium* species, and no Type III and Type IX nsLTPs existed in *G. arboreum*.

Additionally, all the 189 nsLTP sequences were evaluated with OrthoMCL clustering. With the default stringency, 21 orthologous groups (OGs) in 8 subfamilies were shown (Table S3). Each subfamily contained one or more OGs, and each distinct OG was shared by only one specific subfamily. The OG distributions were similar to the phylogenetic classifications of the nsLTP family in the three *Gossypium* species. The protein structures were highly diverse in all the identified nsLTPs (Table S1). The amino acid lengths of the nsLTPs in the Type I, Type V and Type VIII subfamilies were relatively longer, while the proteins in Type II and Type III had relatively shorter amino acid lengths. A similar distribution in the molecular weight of the nsLTPs also existed.

Conserved protein motifs and exon/intron structure of nsLTPs. The main characteristic of plant nsLTPs is the presence of 8 CM in highly conserved positions. Using the WebLogo program, the sequence logos of the identified nsLTPs in *Gossypium* were generated to further confirm the conservation of amino acid residues (Fig. 2). Moreover, a variable number of inter-cysteine amino acid residues was displayed through multiple alignments, and 8 nsLTP types were therefore identified based on the typical spacing of the 8 CM (Table 1). Between the conserved Cys₁ and Cys₂ residues, Type II and VIII nsLTPs contained 6–8 residues, while Type V and IX contained 14 and 13 residues, respectively. Between the conserved Cys₄ and Cys₅ residues, Type I nsLTPs contained 19–20 residues, while the other types contained relatively fewer residues (8–12). Between the conserved Cys₆ and Cys₇ residues, Type III nsLTPs contained 12 residues, while the other types contained more residues (19–27). Between the conserved Cys₇ and Cys₈ residues, Type I nsLTPs contained more residues (13–15) than Type III and Type IX nsLTPs (6).

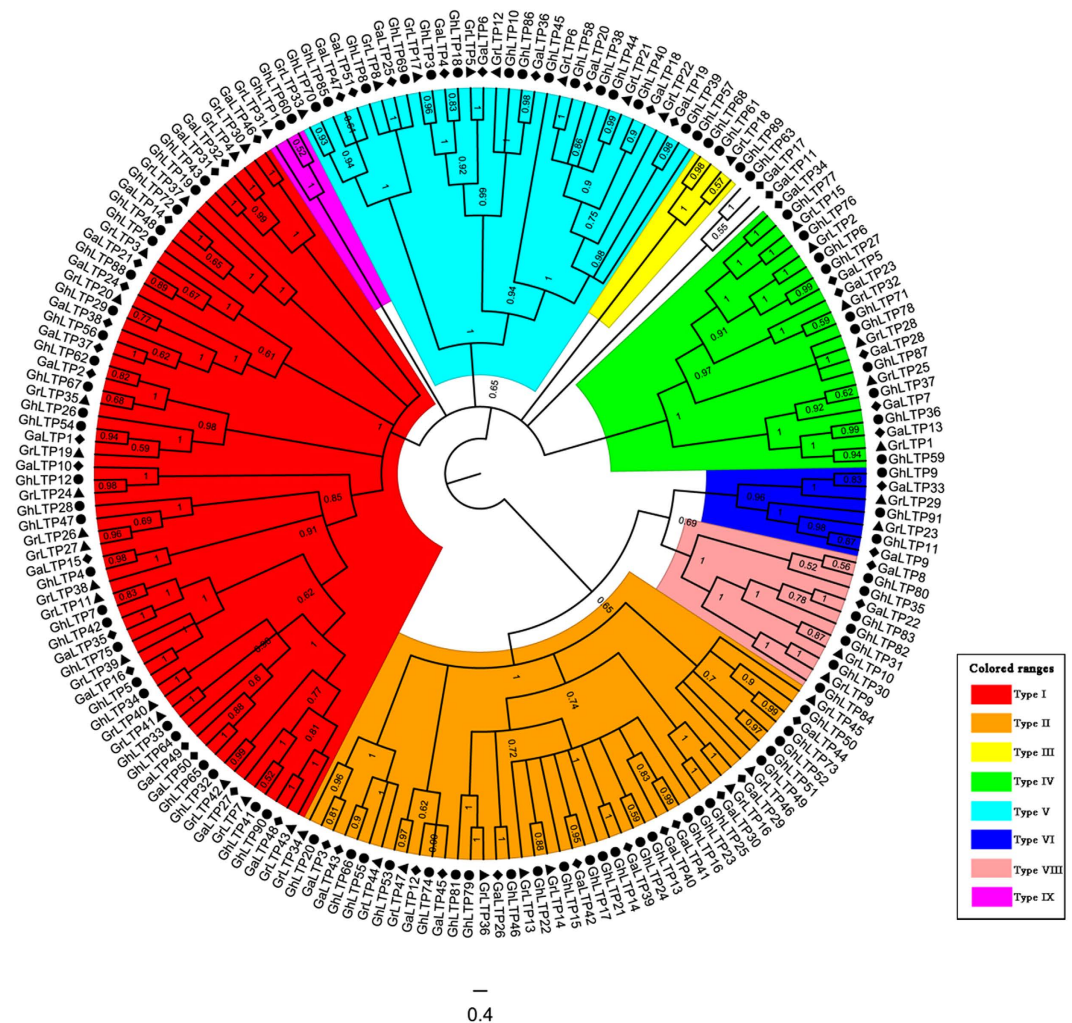


Figure 1. Phylogenetic relationships of the *nsLTP* family from *G. raimondii*, *G. arboreum* and *G. hirsutum*. The phylogenetic tree was generated using the Bayesian method based on multiple alignments of the *nsLTP* sequences. The numbers in the clades are posterior probability values. The *nsLTP* subfamilies are indicated by different colors.

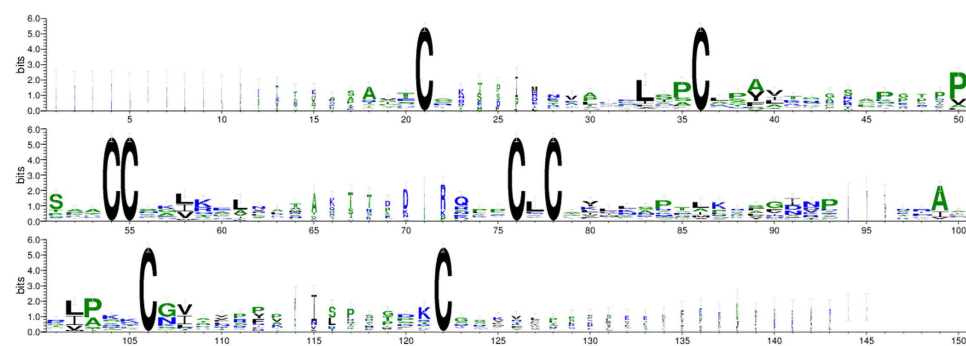


Figure 2. Conserved domain analysis of the *nsLTP*s using the WebLogo program. The height of the letter designating the amino acid residue at each position represents the degree of conservation. The numbers on the x-axis represent the sequence positions in the corresponding conserved domains. The y-axis represents the information content measured in bits.

The MEME motif search tool was employed to identify 20 distinct conserved motifs in the *nsLTP*s (Fig. 3). Based on the distribution of the predicted motifs, the 189 *nsLTP*s were categorized into 8 distinct subfamilies,

Type	Number of members	Spacing pattern												
		X _{2-5,7,9}	C	X ₉	C	X ₁₃₋₁₆	CC	X _{19,20}	CXC	X _{19,21-24}	C	X ₁₃₋₁₅	C	X _{2-5,7,8,10,19-21,23,25}
Type I	63	X _{2-5,7,9}	C	X ₉	C	X ₁₃₋₁₆	CC	X _{19,20}	CXC	X _{19,21-24}	C	X ₁₃₋₁₅	C	X _{2-5,7,8,10,19-21,23,25}
Type II	44	X _{2,5,6,8-11,13,14}	C	X _{7,8}	C	X ₁₂₋₁₄	CC	X ₈	CXC	X ₂₃	C	X _{6,7,9}	C	X ₀
Type III	4	X _{2,8}	C	X ₉	C	X ₁₆	CC	X ₉	CXC	X ₁₂	C	X ₆	C	X _{1,2,4}
Type IV	22	X _{3,6}	C	X ₉	C	X _{15,17}	CC	X ₉	CXC	X _{22,24}	C	X _{7,9}	C	X _{0,2,7,11,12}
Type V	32	X _{3,7}	C	X ₁₄	C	X ₁₄	CC	X _{11,12}	CXC	X ₂₄	C	X ₁₀	C	X _{3,4,6,7,12,14,17,19,23}
Type VI	7	X _{1,5,6,9}	C	X ₁₀	C	X _{12,16}	CC	X ₉	CXC	X ₂₂	C	X ₉	C	X _{6,8-11}
Type VIII	11	X _{3,4,8}	C	X ₆	C	X ₁₄	CC	X ₁₂	CXC	X _{25,27}	C	X ₈	C	X _{6,13,16,20,21,24,37}
Type IX	3	X ₂	C	X ₁₃	C	X ₁₅	CC	X ₉	CXC	X ₂₂	C	X ₆	C	X ₄

Table 1. Diversity of eight cysteine motifs in different types of nsLTPs identified in *Gossypium*. Character “X” represents any amino acid, and the Arabic numeral following “X” stands for the number of amino acid residues.

which was consistent with the classification from the phylogenetic analysis. All the nsLTPs had either Motif 4 or 3, which represented Cys₂. Motif 13, 11 and 14 corresponded to Cys₁, and Motif 7, 18, 19, 6 and 15 mapped to Cys₃Cys₄. In addition, Motif 8, 9, 5, 1 and 12 corresponded to Cys₇ and Cys₈. Motif 1, 2, 6, 10 and 15 mapped to Cys₅XCys₆, and different residues were found in the central position of the Cys₅XCys₆ motif. Seven hydrophilic residues (Arg, Gly, Glu, Asp, Gln, Ser and Lys) and five hydrophobic residues (Tyr, Phe, Leu, Val and Met) existed at the X position of the Cys₅XCys₆ motif in the 189 nsLTPs. Moreover, some subfamily-specific motifs were identified. For instance, Motif 5, 7 and 10 were only present in Type I nsLTPs, and Motif 15 only existed in Type VI nsLTPs.

The gene structure of the nsLTP family was also investigated (Fig. 3). Our results revealed low diversity in the distribution of intronic regions amid the exonic sequences. The intron patterns, formed by relative position and phase, were highly conserved within each phylogenetic group. The number of introns per gene varied from 0 to 2. No introns were identified in Type II and Type III nsLTPs, while some nsLTPs in other subfamilies were interrupted by 1–2 introns positioned 15 to 78 bp downstream of the codon, which almost encoded the Cys₈ in the 8 CM.

Chromosomal localization and duplication of nsLTPs in cotton. Based on the genomic location of nsLTPs (Table S2), chromosomal distribution diagrams of the nsLTP family were generated for the three *Gossypium* species (Fig. 4). In *G. arboreum*, the 51 nsLTPs were distributed unevenly on 12 chromosomes, and the number of nsLTPs on each chromosome varied widely (Fig. 4a). Chromosome 6 had the largest number of nsLTPs with 11 members, followed by Chromosome 1 with 9 genes. In contrast, only 1 gene was located on Chromosome 5, and no nsLTPs were found in Chromosome 2. In *G. raimondii*, the 43 nsLTPs were located on 13 chromosomes, with Chromosome 8 containing the largest number of genes (9) (Fig. 4b). Two genes were present on Chromosome 1, 2, 3, 5 and 9, whereas only a single nsLTP was localized on Chromosome 4, 10 and 12 each. In addition, a total of 30 and 35 nsLTPs were mapped in the 9 A_t and 10 D_t subgenome chromosomes of *G. hirsutum*, respectively (Fig. 4c). D_t-Chromosome 6 contained the maximum number of nsLTPs with 9 genes, followed by A_t-Chromosome 2, D_t-Chromosome 1 and D_t-Chromosome 8 with 6 genes each, while only one gene was present on A_t-Chromosome 13, D_t-Chromosome 5, D_t-Chromosome 7 and D_t-Chromosome 10 each. Besides, no nsLTPs were located on A_t-Chromosome 1, 3, 10 and 12, and D_t-Chromosome 3, 4 and 12. Moreover, several nsLTP clusters were detected on chromosomes such as the top of D_t-Chromosome 6 and the bottom of A_t-Chromosome 2 in *G. hirsutum*.

Gene duplication events were investigated to elucidate the expansion pattern of the nsLTP family in *Gossypium*. In our study, 7, 5 and 6 duplicated gene pairs were identified in *G. arboreum*, *G. raimondii* and *G. hirsutum*, respectively (Table 2). In *G. arboreum* and *G. raimondii*, the duplication events were concentrated in similar subfamilies (including Type I, II and V), whereas in *G. hirsutum* the duplication events occurred in Type II, IV, V and VIII. This result revealed the strong expansion preference for some nsLTP subfamilies in *Gossypium*. Meanwhile, based on the sequence analysis and the chromosomal distribution, 2 and 2 paired genes in *G. arboreum* and *G. hirsutum*, respectively, were identified to be involved in segmental duplication events, while the other 14 pairs were linked to tandem duplication events.

In addition, the Ka/Ks ratio of each duplicated gene pair was calculated to assess the molecular evolutionary rates (Table 2). In this study, 83.3% of the duplicated nsLTPs from cotton have mainly undergone purifying selection pressure after the duplication events (Table 2). As purifying selection apparently constrains the divergence of the duplicated genes, the functions of the duplicated nsLTPs might not diverge much during subsequent evolution. Moreover, the divergence times between the duplicated gene pairs were analyzed. In *G. arboreum* and *G. raimondii*, most of the Ks values were less than 0.17, and their corresponding duplication age might be less than 32.69 million years ago (MYA). Only one duplication event (*GaLTP47/51*) occurred approximately 194.74 MYA. In *G. hirsutum*, the Ks values were 0.03–0.13, and the duplication ages were estimated to be 5.84–24.50 MYA.

Orthologous gene analysis and synteny block detection. The evolution of nsLTPs was analyzed among the three *Gossypium* species. We identified 23 and 24 orthologous gene pairs within the A_t and D_t subgenomes, respectively, in *G. hirsutum* and their corresponding ancestral A and D diploid genomes (Fig. 5, Table S4).

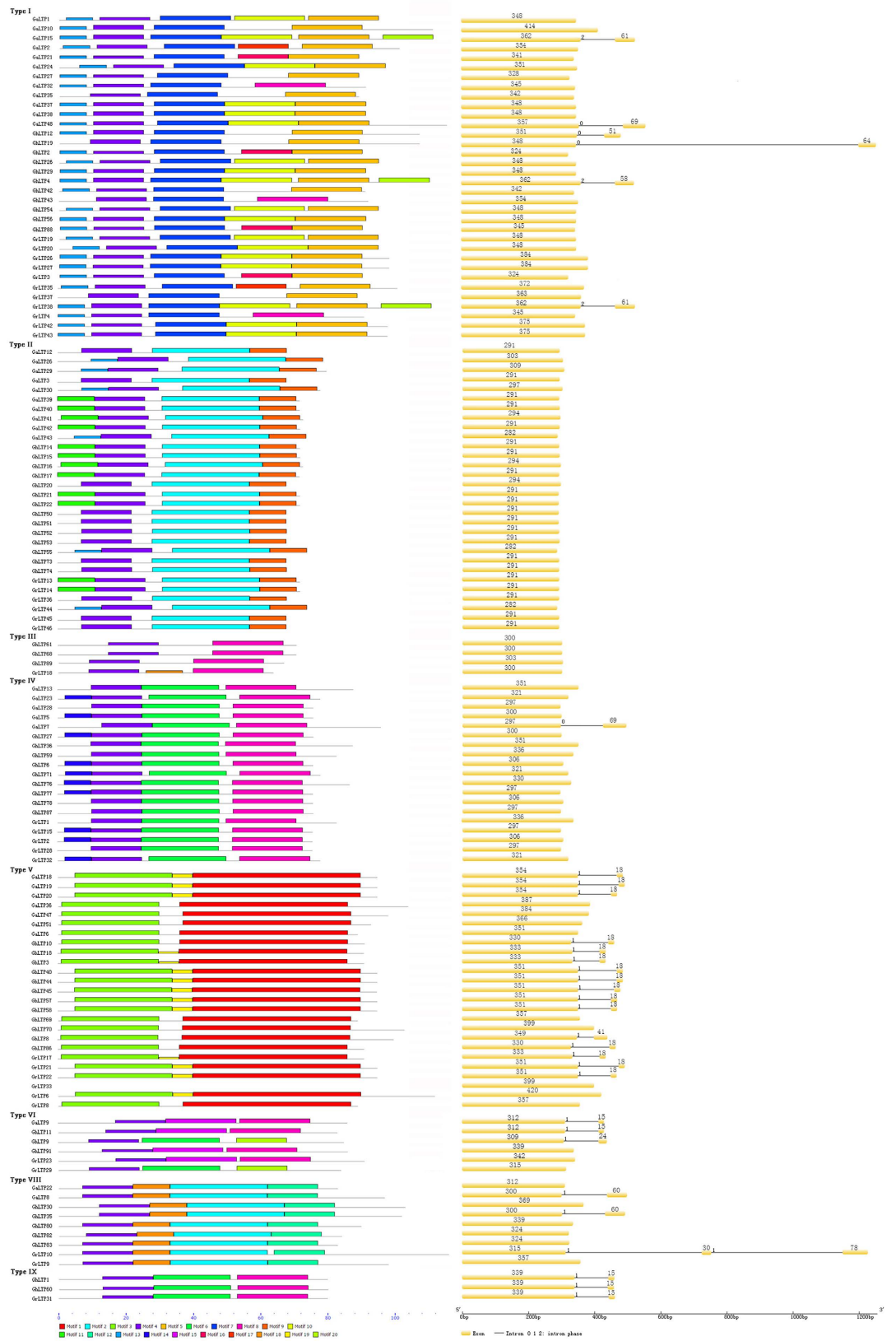


Figure 3. Motif compositions (left panel) and gene structures (right panel) of some nsLTP members in *Gossypium*. The conserved domains were identified using the MEME web server. Different motifs are represented by various colored boxes. The location of each motif can be estimated using the scale at the bottom. Gene structures of nsLTPs were predicted with the GSDS software. The exons are indicated by yellow boxes and the introns are indicated by black lines.

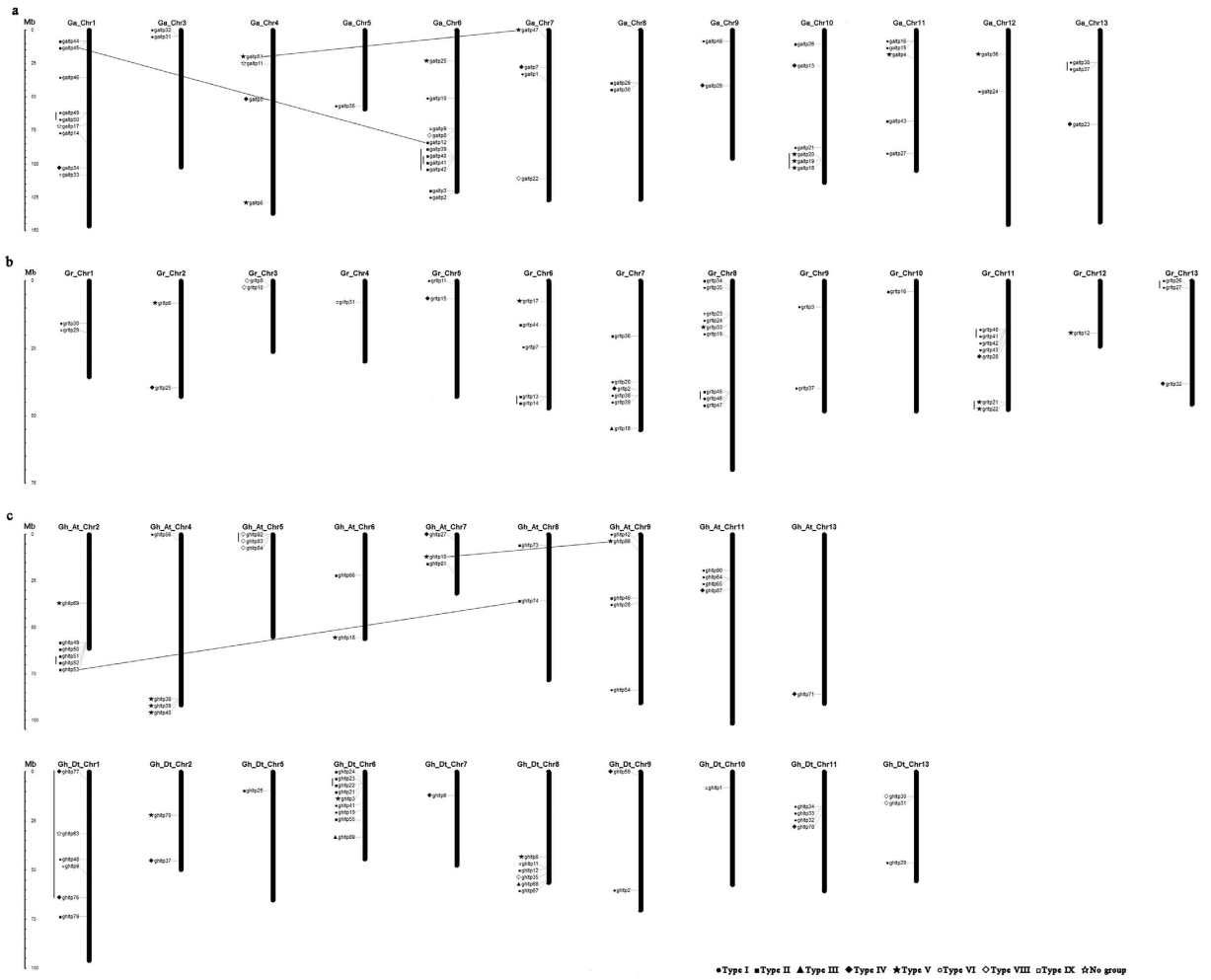


Figure 4. Chromosomal locations of nsLTPs from *G. arboreum* (a) *G. raimondii* (b) and *G. hirsutum* (c). The scale represents megabases (Mb). Chromosome numbers are indicated above each vertical bar. The markers before the gene names indicate the nsLTP subfamily. The duplicated gene pairs are joined by black lines.

Species	Duplicated gene 1	Duplicated gene 2	Subfamily	Ka	Ks	Ka/Ks	Purifying selection	Duplicate type	Age (MYA)
<i>G. arboreum</i>	<i>GaLTP12</i>	<i>GaLTP45</i>	Type II	2.51E-07	5.85E-07	0.42952	Yes	segmental	0.00011255
	<i>GaLTP18</i>	<i>GaLTP20</i>	Type V	0.00737363	0.165432	0.0445719	Yes	tandem	31.8138462
	<i>GaLTP37</i>	<i>GaLTP38</i>	Type I	0.0728347	0.160261	0.454475	Yes	tandem	30.8194231
	<i>GaLTP39</i>	<i>GaLTP42</i>	Type II	0.0312662	0.0690421	0.452857	Yes	tandem	13.2773269
	<i>GaLTP40</i>	<i>GaLTP41</i>	Type II	0.0261638	0.111607	0.234428	Yes	tandem	21.4628846
	<i>GaLTP47</i>	<i>GaLTP51</i>	Type V	0.995287	1.01263	0.982869	Yes	segmental	194.736538
	<i>GaLTP49</i>	<i>GaLTP50</i>	Type I	0.0358127	0.0426301	0.84008	Yes	tandem	8.19809615
	<i>GrLTP13</i>	<i>GrLTP14</i>	Type II	0.0254554	0.128337	0.198347	Yes	tandem	24.6801923
<i>GrLTP21</i>	<i>GrLTP22</i>	Type V	0.0185999	0.164891	0.112801	Yes	tandem	31.7098077	
<i>G. raimondii</i>	<i>GrLTP26</i>	<i>GrLTP27</i>	Type I	2.48E-07	6.24E-07	0.397702	Yes	tandem	0.00011993
	<i>GrLTP40</i>	<i>GrLTP41</i>	Type I	0.0493708	0.0199624	2.47319	No	tandem	3.83892308
	<i>GrLTP45</i>	<i>GrLTP46</i>	Type II	0.00500846	0.000100169	50	No	tandem	0.01926327
	<i>GhLTP10</i>	<i>GhLTP86</i>	Type V	0.0168826	0.0310859	0.543095	Yes	segmental	5.97805769
	<i>GhLTP22</i>	<i>GhLTP23</i>	Type II	0.0148626	0.0889965	0.167002	Yes	tandem	17.1147115
<i>G. hirsutum</i>	<i>GhLTP51</i>	<i>GhLTP52</i>	Type II	0.0187175	0.0303504	0.616713	Yes	tandem	5.83661538
	<i>GhLTP53</i>	<i>GhLTP74</i>	Type II	0.0663427	0.0389369	1.70385	No	segmental	7.48786538
	<i>GhLTP76</i>	<i>GhLTP77</i>	Type IV	0.066261	0.127397	0.520114	Yes	tandem	24.4994231
	<i>GhLTP82</i>	<i>GhLTP83</i>	Type VIII	0.0595669	0.102935	0.578685	Yes	tandem	19.7951923

Table 2. Ka/Ks analysis for the duplicated gene pairs.

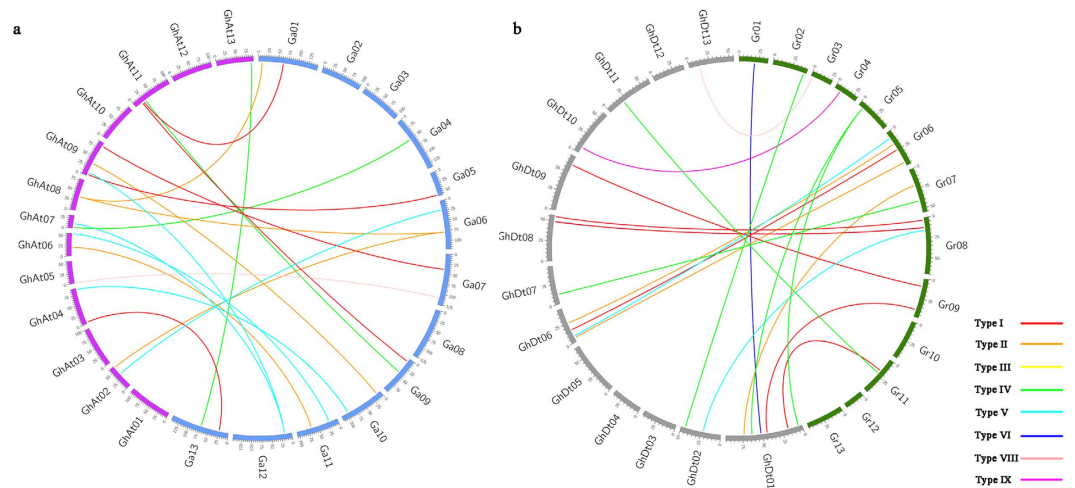


Figure 5. Distribution of *nsLTP* orthologous gene pairs and synteny block identification between the A_t subgenome in *G. hirsutum* and the diploid A genome in *G. arboreum* genome (a) and the D_t subgenome in *G. hirsutum* and the diploid D genome in *G. raimondii* (b). The differently colored lines represent the subfamilies within the *nsLTP* family.

Of the orthologous gene pairs, most were distributed in Type I, II, IV and V (Fig. S3, Table S4). Besides, 24 *GrLTPs* have no orthologs in the D_t subgenome of *G. hirsutum*, and 31 *GaLTPs* have no orthologs in the A_t subgenome. Meanwhile, the K_s values of the orthologous gene sets (A_t vs A and D_t vs D) were also compared. The divergence times between the allotetraploid and its progenitor genomes were estimated to be 3.46–3.54 MYA (K_s peaks at 0.0180 and 0.0184, respectively) (Fig. S4). The similar divergence time suggested that the *nsLTPs* in A_t and D_t subgenomes might have evolved symmetrically.

The conservation and rearrangement of certain chromosome segments may play an important role in the adaptive evolution of the three *Gossypium* species. In our study, we discovered 3 conserved syntenic blocks between the A_t subgenome in *G. hirsutum* and the A diploid genome in *G. arboreum*, and 1 conserved syntenic block between the D_t subgenome in *G. hirsutum* and the D diploid genome in *G. raimondii*. This result indicated that the collinear relationships of the *nsLTPs* between the A_t subgenome and the *G. arboreum* genome were higher than those between the D_t subgenome and the *G. raimondii* genome. These conserved segments contain different numbers of *nsLTPs*, ranging from 2 to 3. According to the analysis, the genes situated on *G. hirsutum* A_t Chromosome 11, 4 and 5 were predicted to have corresponding orthologs on *G. arboreum* Chromosome 1, 10 and 7, respectively, whereas the genes on *G. hirsutum* D_t Chromosome 11 were found to originate from the conserved block on *G. raimondii* Chromosome 11 (Fig. 5). In particular, six paired *nsLTPs* (*GhLTP64/GaLTP49*, *GhLTP65/GaLTP50*, *GhLTP38/GaLTP20*, *GhLTP39/GaLTP19*, *GhLTP82/GaLTP22* and *GhLTP83/GaLTP22*) were located in genomic regions with synteny between the *G. hirsutum* and *G. arboreum* genomes, while three paired *nsLTPs* (*GhLTP32/GrLTP42*, *GhLTP33/GrLTP41* and *GhLTP34/GrLTP40*) were located in genomic regions with synteny between the *G. hirsutum* and *G. raimondii* genomes.

Analysis of orthologous gene expression patterns in cotton. In the current study, expression patterns of the orthologous genes were compared in *G. raimondii*, *G. arboreum* and *G. hirsutum* (Figs 6 and 7 and Fig. S5). Among the intraspecific orthologous genes, 5 paired genes (*GaLTP47/51*, *GaLTP49/50*, *GhLTP10/86*, *GhLTP53/74* and *GrLTP40/41*) shared almost equivalent expression patterns in the tested tissues and leaves inoculated with *V. dahliae* (Fig. 6). However, this was not the case for *GhLTP82/83*, *GrLTP13/14* and *GrLTP21/22*. The expression patterns of these duplicated gene pairs were strongly divergent. *GhLTP83* and *GrLTP14* showed predominant expression in stems compared with *GhLTP82* and *GrLTP13*, respectively. *GrLTP21/22* also showed reciprocal silencing in roots and stems. Apart from the tissue-specific expression biases, *GhLTP82/83* and *GrLTP13/14* showed similar expression profiles after *V. dahliae* infection, while *GrLTP21/22* displayed reverse expression pattern in response to *V. dahliae*.

Among the interspecific orthologous genes, 10 pairs between *G. hirsutum* and *G. arboreum* and 6 pairs between *G. hirsutum* and *G. raimondii* were selected to evaluate their expression relationship (Fig. 7, Fig. S5). Among them, the 4 paired genes (*GaLTP25/GhLTP69*, *GaLTP35/GhLTP42*, *GaLTP36/GhLTP86* and *GaLTP36/GhLTP10*) shared similar expression patterns, and both genes were up-regulated after *V. dahliae* infection. However, the other 12 pairs displayed strong expression bias towards one copy in different organs, and the responses to *V. dahliae* were drastically different (Fig. 7, Fig. S5).

Expression profile of *nsLTP* members in cotton. In the current study, a total of 78 genes (16 *GaLTPs*, 19 *GrLTPs* and 43 *GhLTPs*) from all the subfamilies were selected, and the expression patterns of these genes varied significantly in different tissues (Fig. 8). Generally, Type V *nsLTPs* were mainly expressed at high levels in roots and young stems, while *nsLTPs* in Type I, II, IV and IX were predominantly expressed in stems and leaves. Additionally, *nsLTPs* play an important role in the protective mechanisms against pathogens in plants. The *nsLTPs*

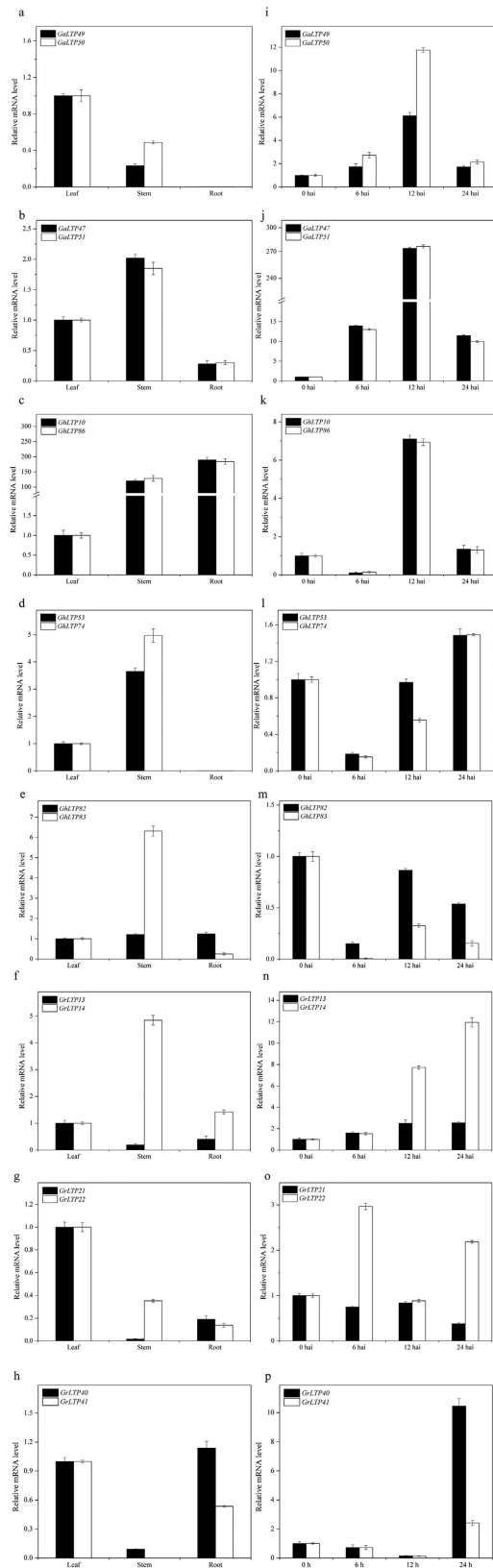


Figure 6. Quantitative RT-PCR analysis for selected duplicated *nsLTPs* from *G. arboreum*, *G. raimondii* and *G. hirsutum* in different organs (a–h) and leaves after *V. dahliae* treatment (i–p).

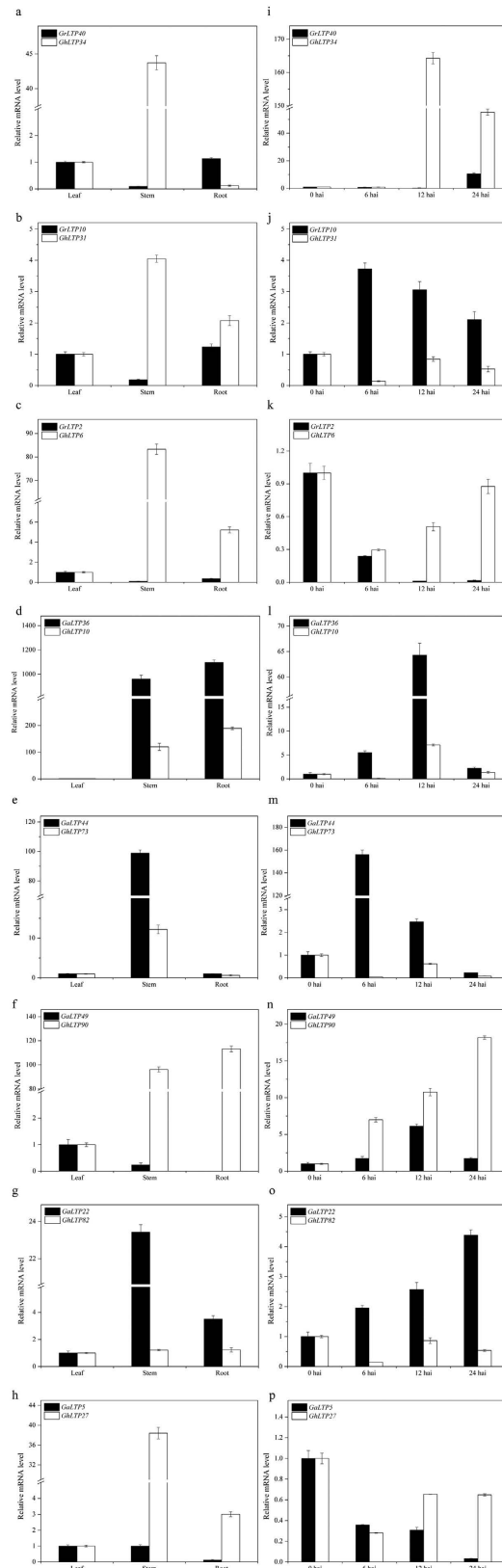


Figure 7. Expression patterns of the orthologous gene pairs from *G. arboreum*, *G. raimondii* and *G. hirsutum* in different organs (a–h) and leaves after *V. dahliae* treatment (i–p).

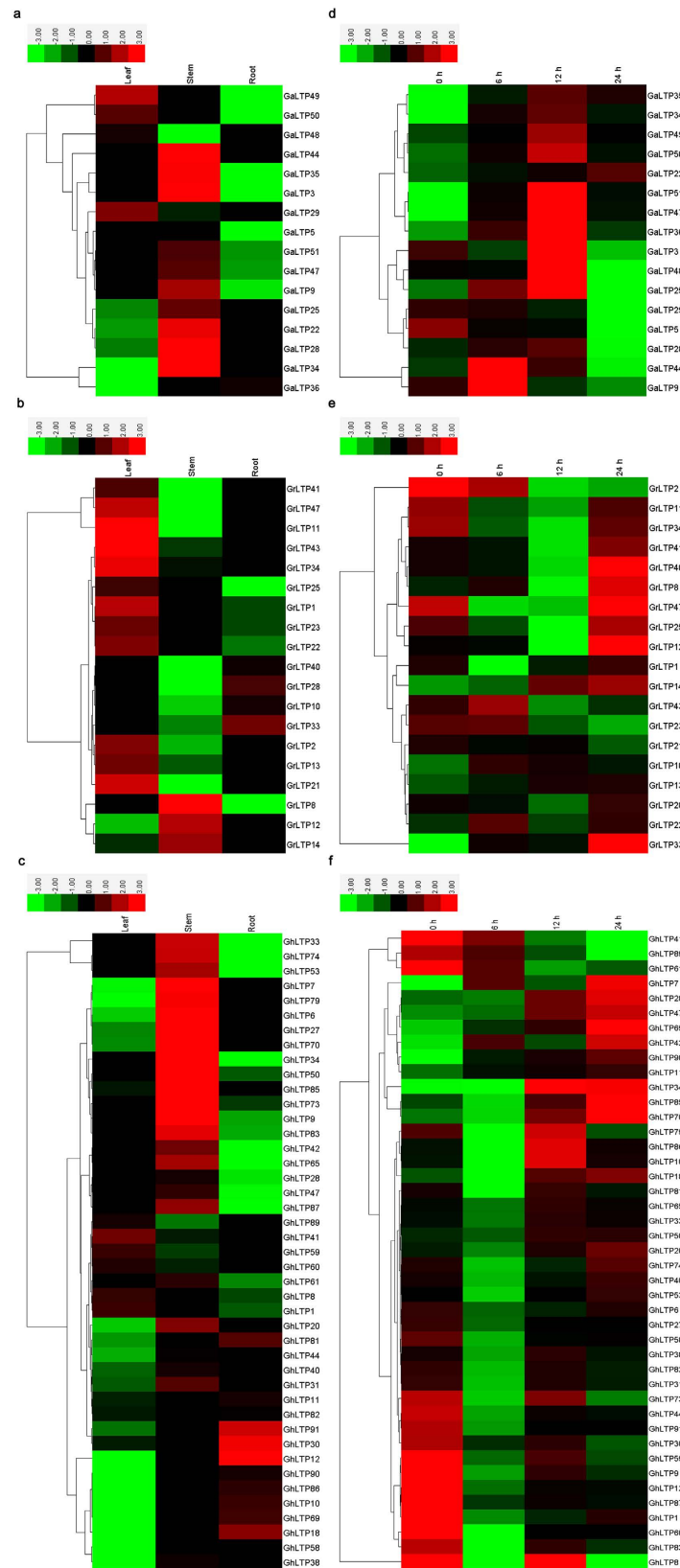


Figure 8. Heat map representation and hierarchical clustering of *GalTLPs*, *GrLTLPs* and *GhLTLPs* across different tissues (a–c) and in leaves after *V. dahliae* treatment (d–f). The color bar represents the relative signal intensity value.

from some plants have reported to show obvious antifungal activities against *V. dahliae*^{24–27}, we thus investigated the expression patterns of the *nsLTPs* in response to *V. dahliae* to take a further step towards understanding the function of cotton *nsLTPs* against *V. dahliae*. As displayed in Fig. 8, most *nsLTPs* in Type I and V showed a marked increase in transcript levels after *V. dahliae* inoculation, and different genes responded to different stages of *V. dahliae* infection. Some Type II *nsLTPs* were also slightly up-regulated in response to *V. dahliae* stress, while some *nsLTPs* in Type III, IV, VI, VIII and XI showed a decline in expression levels after treatment with *V. dahliae*.

Discussion

The categorization of *nsLTPs* based on phylogenetic clustering provided comprehensive information about the gene family and facilitated further functional analysis. In the current study, the 189 *nsLTPs* identified in *G. raimondii*, *G. arboreum* and *G. hirsutum* were classified into 8 subfamilies (Type I, II, III, IV, V, VI, VIII and IX) through phylogenetic analysis, and no Type VII *nsLTPs* were found in *Gossypium* (Fig. 1, Fig. S1). It has been speculated that Type VII *nsLTPs* appeared specifically in monocots while Type IX *nsLTPs* were unique to dicots^{3,9}, and our results in *Gossypium* further confirmed this viewpoint. In addition, *G. arboreum* lost all the Type III and Type IX *nsLTPs* (Fig. S2), suggesting that the evolution of plants not only involves gene retentions, but also is accompanied by gene losses and mutations^{4,28}. Meanwhile, the proportion of *nsLTPs* in each subfamily indicated that Type I seemed to have contracted while Type VIII expanded in *G. hirsutum* compared with its diploid progenitors (Fig. S2b). The gene retentions and losses might be associated with the related functions during plant evolution²⁹.

As for multigene families, the analysis of gene expression profiles often provides useful clues for functional assessment. The tissue-specific expression patterns of *nsLTPs* (Fig. 8) indicated their important roles in performing diverse developmental and physiological functions in cotton. Besides, Type I *nsLTPs* were reported to be involved in plant defense against phytopathogens^{4,10,30}, and were classified as PR-14 family. Such a role is particularly consistent with our results (Fig. 8). Most Type I *nsLTPs* showed increased expression levels after *V. dahliae* infection. In addition, many Type V *nsLTPs* were also significantly induced after *V. dahliae* attack, suggesting that they may participate in the pathogen response. In a previous study, the expression of Type V *nsLTPs* was observed primarily in the vascular bundles, and they were deduced to be involved in defense signaling¹⁰. Additional work is needed to further characterize the role of Type V *nsLTPs* and their functional involvement in signal transduction. Moreover, the *nsLTPs* in other subgroups showed no expression changes or a decline of expression levels when treated with *V. dahliae*, suggesting that they may participate in other biological processes or respond to the attacks of other types of pathogens^{3,4,30–32}.

Most *nsLTPs* within each subgroup shared common motif compositions, and the motif distributions among the different cotton species did not vary much (Fig. 3). Motif 5 and 7 corresponded to the highly conserved residues located in Pro-Tyr-X-Ile-Ser and Thr/Ser-X1-X2-Asp-Arg/Lys, respectively, and the two consensus pentapeptides were only found in Type I *nsLTPs*. Our result is consistent with previous studies^{4,33}. Besides, the properties of the amino acid may determine the Cys pairing style, thus influencing the overall folding of the protein^{30,32,34}. Generally, *nsLTP1* has a hydrophilic amino acid in the CXC motif, whereas *nsLTP2* contains a hydrophobic residue in the same position^{30,32}. In our study, Motif 10 represented the pattern with a hydrophilic residue separating Cys₅ and Cys₆ in Type I, while Motif 1, 2, 6 and 15 corresponded to the Cys₅X₆Cys₆ with a hydrophobic residue in the central position in the other subfamilies. Among the five hydrophobic residues in the CXC motif, Leu is the most frequent residue (75.40%), and this result is in accordance with previous studies^{3,4}. Besides, Cys₅-Val-Cys₆, which corresponded to Motif 15, was only found in four Type VI *nsLTPs*.

The intron-exon pattern carries the imprint of the evolution of a gene family^{35,36}. Previous studies have indicated the generality that some *nsLTPs* in Type I, III, IV, V and VI contained introns, while no introns were identified in Type II, VIII and IX *nsLTPs*^{3,4,32}. However, our result showed some differences. In *Gossypium*, introns were found in Type VIII and IX, while no introns were identified in Type III (Fig. 3). The *nsLTP* family evolved in early diverged land plants, and new subfamilies evolved during land plant evolution^{2,32}. Intron loss events were considered the main cause for the formation of novel *nsLTP* types, and also contributed to novel gene formation within the specific gene subfamilies³². Therefore, compared with the *nsLTPs* in other plants, Type IX and some Type VIII *nsLTPs* in *Gossypium* still possessed introns, while Type III genes have evolved with no introns harbored. The adoption of different *nsLTP* types could help evolved plants adapt to the stressful conditions on land gradually, so the *nsLTP* family was selected and expanded in land plants^{2,32}.

The role of gene duplication in the genesis of evolutionary novelty and complexity has long been recognized^{37,38}. The results in our study indicated that both tandem and segmental duplication events contributed to the expansion of the *nsLTP* family in *G. arboreum* and *G. hirsutum*, while tandem duplication contributed to the *nsLTP* expansion in *G. raimondii* (Fig. 4, Table 2). Previous studies have indicated that the ancient and recent whole-genome duplication (WGD) events occurred in *Gossypium* approximately 115–146 and 13–20 MYA, respectively, and the predicted hybridization and formation of allotetraploid cotton occurred approximately 1.5 MYA^{14,15,23}. In the current study, most of the *nsLTP* duplication events in *G. arboreum* and *G. raimondii* might have occurred fewer than 32.69 MYA, and were considered the recent duplication events. The duplication event occurred 194.74 MYA in *G. arboreum* was therefore regarded as the ancient hexaploidization event. In *G. hirsutum*, the duplication events occurred approximately 5.84–24.50 MYA, suggesting that these duplication events might have occurred before the interspecific hybridization and subsequent polyploidization in *G. hirsutum*.

In addition, the orthologous genes in *G. arboreum*, *G. raimondii* and *G. hirsutum* were identified (Fig. 5, Table S4). The results revealed that 31 *GaLTPs* lost their orthologs in the A_t subgenome of *G. hirsutum* and 24 *GrLTPs* lost their orthologs in the D_t subgenome. These genes were mainly distributed in Type I, Type II, Type IV and Type V, and the proportions of these *GrLTP* and *GaLTP* genes distributed in each subfamily were complementary (Fig. S3). For example, in Type I, 66.67% of the *GaLTPs* had no orthologs in the A_t subgenome, whereas a relatively lower ratio (50%) of the *GrLTPs* lost their orthologs in the D_t subgenome. On the contrary, in Type

V, only 33.33% of the *GaLTPs* lost their orthologs, while many more *GrLTPs* (75%) lost their orthologs. The ratios in other subfamilies such as Type IV, VI and VIII showed similar complementary phenomena, suggesting that the loss and retention of *nsLTPs* in *G. hirsutum* might not be random. During the process of polyploidization, chromosomal recombinations and rearrangements resulted in gene losses and gene retentions as duplicate orthologs^{39,40}. The regular losses in conjunction with retentions might have avoided severe functional loss and redundancy of the genes in plants.

Duplications of genomic content often occur during DNA replication and recombination through independent mechanisms^{38,41}. Some duplicated genes might have been subjected to diversification of their functions due to the divergent changes in their protein sequences together with *cis*-regulatory elements³⁷. The *nsLTPs* may have undergone independent duplication events followed by functional diversification in each species during speciation^{42,43}. In rice and wheat, the *nsLTPs* may have suffered from a complex evolutionary selection mechanism including subfunctionalization^{43,44}. The functional diversification of *nsLTPs* appears to be not random, but seems to have originated from the specific biological processes over the course of evolution. In the current study, five pairs of duplicated genes shared similar expression profiles (Fig. 6). These results indicated that these duplicated genes might retain some essential functions during subsequent evolution, and the similar expression patterns may be related to the highly similar protein architecture of these duplicated genes. However, three paired duplicated genes showed significant expression divergence (Fig. 6). The diversity might be caused by the significant variation in gene regulation after the duplication events^{45,46}. The differential expression patterns of duplicated genes in *Gossypium* demonstrated that these genes might have experienced functionalization during the evolutionary process.

As a prominent mode of speciation in flowering plants, allopolyploidy can cause genomic changes, including chromosomal rearrangements and changes in gene expression^{45–48}. Recent studies have indicated the unequal expression of orthologous genes in allotetraploids such as *Gossypium*^{13,49}, *Brassica*⁴⁷, *Oryza minuta*⁵⁰ and the synthetic allopolyploid *Arabidopsis*⁵¹, and the gene expression levels in these allopolyploids deviated from the expression of their orthologous genes in the progenitors. In our study, the expression patterns of genes in *G. hirsutum* revealed considerable differences from the expression of their orthologous genes in its progenitors (Fig. 7 and Fig. S5), indicating that the functions of the orthologous genes were strongly differentiated over the course of evolution.

In summary, 189 *nsLTPs* were identified in *G. raimondii*, *G. arboreum* and *G. hirsutum* in this study. Comprehensive study of the *nsLTPs* in *Gossypium* provided some important features of the gene family such as gene structure, expansion and expression. The findings here provide researchers with novel findings about the molecular evolution and expansion history of the *nsLTP* family in *Gossypium*, and offer a good opportunity to further investigate the *nsLTP* family in plants, especially polyploid plants. Besides, the analysis of the cotton *nsLTPs* in response to *V. dahliae* might help guide future identification of disease-resistant genes and exploitation of wilt-resistant varieties.

Materials and Methods

Plant materials and *V. dahliae* spore treatment. The seeds of *G. raimondii*, *G. arboreum* (Shixiya1) and *G. hirsutum* (TM-1) were kindly supplied by National Medium-term Gene Bank of Cotton in China. Cotton seeds were surface-sterilized with 0.1% HgCl₂ for 10–15 min and washed with sterile water for at least 5 times. Sterilized seeds were sown on the half-strength Murashige and Skoog (MS) solid medium. After 3-day germination, the seedlings were transferred to half-strength Hoagland nutrient solution at pH 6.0. Fresh nutrient solution was continuously aerated with pumps and air stones, and was changed every 3 days. Plants were cultivated in a growth chamber at 28 °C with a photoperiod of 16 h light and 8 h dark. For tissue-specific expression analysis, roots, stems and leaves were harvested from 3-week-old cotton seedlings, and quick-frozen in liquid nitrogen, then stored at –80 °C until RNA isolation. Three plants constituted an individual replicate and three biological replicates were sampled for RNA extraction.

V. dahliae isolate Anyang (ACCC no. 36207) is a popular *V. dahliae* strain isolated from Anyang, Henan Province, China. It was supplied by the Cotton Research Institute of the Chinese Academy of Agricultural Science and preserved at the Agricultural Culture Collection, Beijing, China. *V. dahliae* mycelia growing on potato dextrose agar (PDA) plates were transferred to Czapek's medium (containing 2.0 g·l⁻¹ NaNO₃, 1.0 g·l⁻¹ K₂HPO₄, 0.5 g·l⁻¹ MgSO₄·7H₂O, 1.0 g·l⁻¹ KCl, 0.01 g·l⁻¹ FeSO₄·7H₂O and 30.0 g·l⁻¹ sucrose) on a shaker at 150 rpm at 25 °C for sub-culturing. The spore concentration was determined with a haemocytometer and adjusted to a concentration of 10⁷ spores ml⁻¹ with sterile distilled water prior to use. Three-week old plants were inoculated with *V. dahliae* spores using the root-dip method, and the leaves were collected 0 h, 6 h, 12 h and 24 h after *V. dahliae* inoculation to examine the expression patterns of the *nsLTP* family in cotton under *V. dahliae* treatment.

RNA isolation and quantitative real-time PCR (qRT-PCR). Total RNA was extracted using an RNAPrep Pure Plant kit (Tiandz, China), and first-strand cDNA was synthesized from DNase-treated RNA with a PrimerScript 1st Strand cDNA synthesis kit (TaKaRa). Gene-specific primers were designed based on their coding sequences (CDSs) and then synthesized commercially (Generay, Shanghai, China) (Table S5). qRT-PCR was performed with SYBR premix Ex Taq (TaKaRa) and the CFX96 Realtime System (Bio-Rad, France) by strictly following the manufacturer's instructions. The qRT-PCR machine was programmed with 40 cycles and an annealing temperature of 60 °C. The cotton *EF1α* gene was used as an endogenous control for all the qRT-PCR analyses. The relative transcription levels were calculated using the 2^{-ΔΔCT} method. Three technical replicates were performed for each sample. The expression profiles of the *nsLTPs* were clustered using Cluster 3.0 software⁵².

Sequence retrieval and structural analysis. All the *nsLTP* sequences of *Arabidopsis* (Table S1) were collected from TAIR (<http://www.arabidopsis.org/index.jsp>) and were used as queries by searching against the cotton

genome database^{14,15,23} using the BLASTP program with default parameters ($E_value \leq 10$) (<http://cgp.genomics.org.cn/page/species/index.jsp>). The conserved LTP domain of each putative LTP sequence in *Gossypium* was confirmed in the Conserved Domain Database in National Center for Biotechnology Information (NCBI) (<http://www.ncbi.nlm.nih.gov>). Then, the candidate nsLTP sequences were manually examined for the presence of the 8 CM, and proteins lacking the essential Cys residues were excluded. After that, the putative proline-rich proteins and the proteins without NSSs (checked with SignalP 4.0, <http://www.cbs.dtu.dk/services/SignalP>) were also removed. Additionally, the proteins with C-terminal GPI anchor signals (predicted with big-PI Plant Predictor, PSORT and PredGPI) were excluded^{53–55}. The protein sequences of the 2S- albumins (At2S1 to At2S4)⁵⁶ and alpha amylase inhibitor (RATI)⁵⁷ were then BLAST-searched against the rest of the candidate nsLTPs to exclude possible inhibitors and cereal storage proteins. Moreover, the proteins with more than 120 amino acids at maturity were discarded. Through these searching and screening procedures, the rest of the nsLTPs were finally confirmed and used for the following analysis. Primary and secondary protein structures were predicted with ProtParam (<http://web.expasy.org/protparam/>) and SOPMA (http://npsa-pbil.ibcp.fr/cgi-bin/npsa_automat.pl?page=npsa_sopma.html). In addition, the nsLTPs were clustered using OrthoMCL to identify the orthologous groups (OGs)⁵⁸. The inflation parameter was set to the default.

Phylogenetic analysis and sequence alignment. All the nsLTP sequences in this study were aligned using ClustalX version 2.1⁵⁹. The PHYLIP program (<http://evolution.genetics.washington.edu/phylip.html>) was used to estimate the maximum-likelihood phylogeny for all the nsLTP sequences in Arabidopsis and the three *Gossypium* species with the JTT model. In addition, MrBayes version 3.1.2 was used to conduct Bayesian analysis for the nsLTP sequences in the three *Gossypium* species⁶⁰. Trees were visualized with Figtree version 1.4.0 (<http://tree.bio.ed.ac.uk/software/figtree/>).

Protein motif and gene structure analysis. The conserved motifs of the nsLTPs were investigated using the online MEME program⁶¹. The analysis was performed with a set of parameters as follows: the optimum motif width was set to ≥ 6 and ≤ 200 ; the maximum number of motifs was set to 20⁶². Sequence logos for the conserved domains were generated using the WebLogo tool (<http://weblogo.berkeley.edu/>). Genomic schematic diagrams of the nsLTPs were obtained by comparing the genomic sequences and their predicted CDSs using the GSDS tool (<http://gsds.cbi.pku.edu.cn/>).

Chromosomal mapping and gene duplications. The chromosome location information of the nsLTPs was searched in the cotton genome database. MapInspect software (<http://www.plantbreeding.wur.nl/uk/software-mapinspect.html>) was used to generate chromosomal distribution images for these nsLTPs in *G. raimondii*, *G. arboreum* and *G. hirsutum*. Gene duplication events were investigated as described in previous reports⁶². Orthologous groups of the nsLTP family among the three *Gossypium* species were generated using the OrthoMCL database. Conserved syntenic blocks were inferred by running the OrthoClusterDB tool available at GDR (<http://genome.sfu.ca/cgi-bin/orthoclusterdb/runortho.cgi>). The diagram was plotted using Circos⁶³. Furthermore, the selection pressure for each orthologous gene pair was calculated by the Ka (non-synonymous substitution rate)/Ks (synonymous substitution rate) ratio⁶⁴. The formula " $t = Ks/2r$ " was used to estimate the divergence time, and a neutral substitution rate (r) of 2.6×10^{-9} was used in the current study.

References

- Kader, J. Lipid-transfer proteins in plants. *Annu. Rev. Plant Biol.* **47**, 627–654 (1996).
- Liu, F. *et al.* Non-specific lipid transfer proteins in plants: presenting new advances and an integrated functional analysis. *J. Exp. Bot.* **10.1093/jxb/erv313** (2015).
- Boutrot, F., Chantret, N. & Gautier, M. Genome-wide analysis of the rice and Arabidopsis non-specific lipid transfer protein (nsLTP) gene families and identification of wheat nsLTP genes by EST data mining. *BMC Genomics* **9**, 86, 10.1186/1471-2164-9-86 (2008).
- Li, J. *et al.* Genome-wide survey and expression analysis of the putative non-specific lipid transfer proteins in *Brassica rapa* L. *PLoS ONE* **9**, e84556, 10.1371/journal.pone.0084556 (2014).
- Sels, J., Mathys, J., De Coninck, B. M., Cammue, B. P. & De Bolle, M. F. Plant pathogenesis-related (PR) proteins: a focus on PR peptides. *Plant Physiol. Bioch.* **46**, 941–950 (2008).
- Regente, M. C., Giudici, A. M., Villalain, J. & Canal, L. The cytotoxic properties of a plant lipid transfer protein involve membrane permeabilization of target cells. *Lett. Appl. Microbiol.* **40**, 183–189 (2005).
- Zhu, X. *et al.* Overexpression of wheat lipid transfer protein gene *TaLTP5* increases resistances to *Cochliobolus sativus* and *Fusarium graminearum* in transgenic wheat. *Funct. Integr. Genomic* **12**, 481–488 (2012).
- Jung, H. W., Kim, W. & Hwang, B. K. Three pathogen-inducible genes encoding lipid transfer protein from pepper are differentially activated by pathogens, abiotic, and environmental stresses. *Plant, cell & environment* **26**, 915–928 (2003).
- Liu, W. *et al.* Discovery, identification and comparative analysis of non-specific lipid transfer protein (nsLTP) family in *Solanaceae*. *Genomics, proteomics & bioinformatics* **8**, 229–237 (2010).
- Wang, H. W. *et al.* Insight into the molecular evolution of non-specific lipid transfer proteins via comparative analysis between rice and sorghum. *DNA Res.* **10.1093/dnares/dss003** (2012).
- Wang, N. *et al.* Construction and analysis of a plant non-specific lipid transfer protein database (nsLTPDB). *BMC Genomics* **13**, 1, 10.1186/1471-2164-13-S1-S9 (2012).
- Tapia, G., Morales-Quintana, L., Parra, C., Berbel, A. & Alcorta, M. Study of nsLTPs in *Lotus japonicus* genome reveal a specific epidermal cell member (LjLTP10) regulated by drought stress in aerial organs with a putative role in cutin formation. *Plant Mol. Biol.* **82**, 485–501 (2013).
- Flagel, L. E., Wendel, J. F. & Udall, J. A. Duplicate gene evolution, homoeologous recombination, and transcriptome characterization in allopolyploid cotton. *BMC Genomics* **13**, 302, 10.1186/1471-2164-13-302 (2012).
- Li, F. *et al.* Genome sequence of the cultivated cotton *Gossypium arboreum*. *Nat. Genet.* **46**, 567–572 (2014).
- Li, F. *et al.* Genome sequence of cultivated Upland cotton (*Gossypium hirsutum* TM-1) provides insights into genome evolution. *Nat. Biotechnol.* **33**, 524–530 (2015).
- Wendel, J. F., Schnabel, A. & Seelanan, T. Bidirectional interlocus concerted evolution following allopolyploid speciation in cotton (*Gossypium*). *P. Nat. Acad. Sci.* **92**, 280–284 (1995).

17. Paterson, A. H. *et al.* Repeated polyploidization of *Gossypium* genomes and the evolution of spinnable cotton fibres. *Nature* **492**, 423–427 (2012).
18. Zhang, W. W. *et al.* Cotton gene expression profiles in resistant *Gossypium hirsutum* cv. Zhongzhimian KV1 responding to *Verticillium dahliae* strain V991 infection. *Mol. Biol. Rep.* **39**, 9765–9774 (2012).
19. Zhao, Y., Wang, H., Chen, W. & Li, Y. Genetic structure, linkage disequilibrium and association mapping of *Verticillium* wilt resistance in elite cotton (*Gossypium hirsutum* L.) germplasm population. *PLoS ONE* **9**, e86308, 10.1371/journal.pone.0086308 (2014).
20. Chen, J. *et al.* Genome-wide analysis of the gene families of resistance gene analogues in cotton and their response to *Verticillium* wilt. *BMC Plant Biol.* **15**, 148, 10.1186/s12870-015-0508-3 (2015).
21. Feng, J. *et al.* Analysis of five differentially expressed gene families in fast elongating cotton fiber. *Acta Bioch. Bioph. Sin.* **36**, 51–56 (2004).
22. Gao, P. *et al.* Identification of genes preferentially expressed in cotton fibers: A possible role of calcium signaling in cotton fiber elongation. *Plant Sci.* **173**, 61–69 (2007).
23. Wang, K. *et al.* The draft genome of a diploid cotton *Gossypium raimondii*. *Nat Genet.* **44**, 1098–1103 (2012).
24. Cammue, B. P. A. *et al.* A potent antimicrobial protein from onion seeds showing sequence homology to plant lipid transfer proteins. *Plant Physiol.* **109**, 445–455 (1995).
25. Yili, A. *et al.* Fungicidal lipid-transfer peptide from *Daucus carota sativa* seeds. *Chem. Nat. Compd.* **43**, 450–453 (2007).
26. Yang, X., Xiao, Y., Wang, X. & Pei, Y. Expression of a novel small antimicrobial protein from the seeds of motherwort (*Leonurus japonicus*) confers disease resistance in tobacco. *Appl. Environ. Microb.* **73**, 939–946 (2007).
27. Sun, J. Y. *et al.* Characterization and antifungal properties of wheat nonspecific lipid transfer proteins. *Mol. Plant Microbe In.* **21**, 346–360 (2008).
28. Krishnamurthy, P., Kim, J. A., Jeong, M., Kang, C. H. & Lee, S. I. Defining the RNA-binding glycine-rich (RBG) gene superfamily: new insights into nomenclature, phylogeny and evolutionary trends obtained by genome-wide comparative analysis of Arabidopsis, Chinese cabbage, rice and maize genomes. *Mol. Genet. Genomics* **290**, 2279–2295 (2015).
29. Fan, K. *et al.* Molecular evolution and expansion analysis of the NAC transcription factor in *Zea mays*. *PLoS ONE* **9**, e111837, 10.1371/journal.pone.0111837 (2014).
30. Wei, K. & Zhong, X. Non-specific lipid transfer proteins in maize. *BMC Plant Biol.* **14**, 281, 10.1186/s12870-014-0281-8 (2014).
31. Cotta, M. G. *et al.* Lipid transfer proteins in coffee: isolation of *Coffea* orthologs, *Coffea arabica* homeologs, expression during coffee fruit development and promoter analysis in transgenic tobacco plants. *Plant Mol. Biol.* **85**, 11–31 (2014).
32. Edstam, M. M., Viitanen, L., Salminen, T. A. & Edqvist, J. Evolutionary history of the non-specific lipid transfer proteins. *Mol. Plant* **4**, 947–964 (2011).
33. Douliez, J., Michon, T., Elmorjani, K. & Marion, D. Mini review: structure, biological and technological functions of lipid transfer proteins and indolines, the major lipid binding proteins from cereal kernels. *J. Cereal. Sci.* **32**, 1–20 (2000).
34. Douliez, J. P., Pato, C., Rabesona, H., Mollé, D. & Marion, D. Disulfide bond assignment, lipid transfer activity and secondary structure of a 7-kDa plant lipid transfer protein, LTP2. *Eur. J. Biochem.* **268**, 1400–1403 (2001).
35. Lynch, M. Intron evolution as a population-genetic process. *P. Nat. Acad. Sci.* **99**, 6118–6123 (2002).
36. Del Campo, E. M., Casano, L. M. & Barreno, E. Evolutionary implications of intron-exon distribution and the properties and sequences of the *RPL10A* gene in eukaryotes. *Mol. Phylogenet. Evol.* **66**, 857–867 (2013).
37. Moore, R. C. & Purugganan, M. D. The evolutionary dynamics of plant duplicate genes. *Curr. Opin. Plant Biol.* **8**, 122–128 (2005).
38. Flagel, L. E. & Wendel, J. F. Gene duplication and evolutionary novelty in plants. *New Phytol.* **183**, 557–564 (2009).
39. Paterson, A. H. *et al.* Many gene and domain families have convergent fates following independent whole-genome duplication events in *Arabidopsis*, *Oryza*, *Saccharomyces* and *Tetraodon*. *Trends Genet.* **22**, 597–602 (2006).
40. Buggs, R. J. *et al.* Rapid, repeated, and clustered loss of duplicate genes in allopolyploid plant populations of independent origin. *Curr. Biol.* **22**, 248–252 (2012).
41. Ramsey, J. & Schemske, D. W. Pathways, mechanisms, and rates of polyploid formation in flowering plants. *Annu. Rev. Eco. Syst.* **29**, 467–501 (1998).
42. Jang, C. S. *et al.* Divergence of genes encoding non-specific lipid transfer proteins in the *Poaceae* family. *Mol. Cells* **24**, 215–223 (2007).
43. Jang, C. S. *et al.* Evolution of non-specific lipid transfer protein (*nsLTP*) genes in the *Poaceae* family: their duplication and diversity. *Mol. Genet. Genomics* **279**, 481–497 (2008).
44. Wang, H. W. *et al.* Expressional diversity of wheat *nsLTP* genes: evidence of subfunctionalization via *cis*-regulatory divergence. *Genetica* **138**, 843–852 (2010).
45. Adams, K. L. Evolution of duplicate gene expression in polyploid and hybrid plants. *J. Hered.* **98**, 136–141 (2007).
46. Wang, J., Tian, L., Lee, H. & Chen, Z. J. Nonadditive regulation of *FRI* and *FLC* loci mediates flowering-time variation in Arabidopsis allopolyploids. *Genetics* **173**, 965–974 (2006).
47. Zhang, X. *et al.* Interspecific hybridization, polyploidization, and backcross of *Brassica oleracea* var. *alboglabra* with *B. rapa* var. *purpurea* morphologically recapitulate the evolution of *Brassica* vegetables. *Sci. Rep.* **6**, 18618, 10.1038/srep18618 (2016).
48. Wang, J. *et al.* Genomewide nonadditive gene regulation in Arabidopsis allotetraploids. *Genetics* **172**, 507–517 (2006).
49. Yoo, M. J., Szadkowski, E. & Wendel, J. F. Homoeolog expression bias and expression level dominance in allopolyploid cotton. *Heredity* **110**, 171–180 (2013).
50. Sui, Y., Li, B., Shi, J. & Chen, M. Genomic, regulatory and epigenetic mechanisms underlying duplicated gene evolution in the natural allotetraploid *Oryza minuta*. *BMC Genomics* **15**, 1, 10.1186/1471-2164-15-11 (2014).
51. Akama, S., Shimizu-Inatsugi, R., Shimizu, K. K. & Sese, J. Genome-wide quantification of homeolog expression ratio revealed nonstochastic gene regulation in synthetic allopolyploid Arabidopsis. *Nucleic Acids Res.* **42**, e46, 10.1093/nar/gkt1376 (2014).
52. de Hoon, M. J., Imoto, S., Nolan, J. & Miyano, S. Open source clustering software. *Bioinformatics* **20**, 1453–1454 (2004).
53. PSORT, I. I. PSORT: a program for detecting sorting signals in proteins and predicting their subcellular localization. *J. Mol. Biol.* **266**, 594–600 (1997).
54. Pierleoni, A., Martelli, P. L. & Casadio, R. PredGPI: a GPI-anchor predictor. *BMC Bioinformatics* **9**, 392, 10.1186/1471-2105-9-392 (2008).
55. Eisenhaber, B. *et al.* Glycosylphosphatidylinositol lipid anchoring of plant proteins. Sensitive prediction from sequence-and genome-wide studies for Arabidopsis and rice. *Plant Physiol.* **133**, 1691–1701 (2003).
56. Guerche, P. *et al.* Differential expression of the Arabidopsis *2S albumin* genes and the effect of increasing gene family size. *Plant Cell* **2**, 469–478 (1990).
57. Alam, N., Gourinath, S., Dey, S., Srinivasan, A. & Singh, T. P. Substrate-inhibitor interactions in the kinetics of α -amylase inhibition by ragi α -amylase/trypsin inhibitor (RATI) and its various N-terminal fragments. *Biochemistry-US* **40**, 4229–4233 (2001).
58. Li, L., Stoeckert, C. J. & Roos, D. S. OrthoMCL: identification of ortholog groups for eukaryotic genomes. *Genome Res.* **13**, 2178–2189 (2003).
59. Larkin, M. A. *et al.* Clustal W and Clustal X version 2.0. *Bioinformatics* **23**, 2947–2948 (2007).
60. Huelsenbeck, J. P. & Ronquist, F. MRBAYES: Bayesian inference of phylogenetic trees. *Bioinformatics* **17**, 754–755 (2001).
61. Bailey, T. L., Johnson, J., Grant, C. E. & Noble, W. S. The MEME Suite. *Nucleic Acids Res.* **43**, W39–W49 (2015).

62. Zhao, Y. *et al.* Systematic analysis of sequences and expression patterns of drought-responsive members of the *HD-Zip* gene family in maize. *PLoS ONE* **6**, e28488, 10.1371/journal.pone.0028488 (2011).
63. Krzywinski, M. *et al.* Circos: an information aesthetic for comparative genomics. *Genome Res.* **19**, 1639–1645 (2009).
64. Zhang, Z. *et al.* KaKs_Calculator: calculating Ka and Ks through model selection and model averaging. *Genomics, proteomics & bioinformatics* **4**, 259–263 (2006).

Acknowledgements

We are greatly grateful to Shuna Yuan and Mi Ni (Zhejiang University, China) for their support in this study. This work was financially supported by the National Natural Science Foundation of China (31171616 and 31471567).

Author Contributions

X.W., F.L. and K.F. conceived and designed research. X.W., F.L., K.F. and E.Y. contributed new reagents or analytical tools. F.L., K.F., F.M. and E.Y. analyzed data. F.L., F.M., M.W. and H.S. conducted experiments. F.L., K.F., N.B., H.M. and X.W. contributed to the writing of the manuscript. All authors read and approved the manuscript.

Additional Information

Supplementary information accompanies this paper at <http://www.nature.com/srep>

Competing financial interests: The authors declare no competing financial interests.

How to cite this article: Li, F. *et al.* Genomic Identification and Comparative Expansion Analysis of the *Non-Specific Lipid Transfer Protein* Gene Family in *Gossypium*. *Sci. Rep.* **6**, 38948; doi: 10.1038/srep38948 (2016).

Publisher's note: Springer Nature remains neutral with regard to jurisdictional claims in published maps and institutional affiliations.



This work is licensed under a Creative Commons Attribution 4.0 International License. The images or other third party material in this article are included in the article's Creative Commons license, unless indicated otherwise in the credit line; if the material is not included under the Creative Commons license, users will need to obtain permission from the license holder to reproduce the material. To view a copy of this license, visit <http://creativecommons.org/licenses/by/4.0/>

© The Author(s) 2016